Bioconjugate Chemistry

Article

pubs.acs.org/bc

Combination of Nanoparticle-Delivered siRNA for Astrocyte Elevated Gene-1 (AEG-1) and All-*trans* Retinoic Acid (ATRA): An Effective Therapeutic Strategy for Hepatocellular Carcinoma (HCC)

Devaraja Rajasekaran,[†,#] Jyoti Srivastava,[†,#] Kareem Ebeid,[‡,#] Rachel Gredler,[†] Maaged Akiel,[†] Nidhi Jariwala,[†] Chadia L. Robertson,[†] Xue-Ning Shen,[†] Ayesha Siddiq,[†] Paul B. Fisher,[†,§,∥] Aliasger K. Salem,*[,‡,⊥] and Devanand Sarkar*[,†,§,∥]

[†]Department of Human and Molecular Genetics, [§]Massey Cancer Center; and [∥]VCU Institute of Molecular Medicine (VIMM), Virginia Commonwealth University, Richmond, Virginia 23298, United States

[‡]Department of Pharmaceutical Sciences and Experimental Therapeutics, College of Pharmacy, and [⊥]Holden Comprehensive Cancer Center, University of Iowa, Iowa City, Iowa 52242, United States

ABSTRACT: Hepatocellular carcinoma (HCC) is a fatal cancer with no effective therapy. Astrocyte elevated gene-1 (AEG-1) plays a pivotal role in hepatocarcinogenesis and inhibits retinoic acid-induced gene expression and cell death. The combination of a lentivirus expressing AEG-1 shRNA and all-*trans* retinoic acid (ATRA) profoundly and synergistically inhibited subcutaneous human HCC xenografts in nude mice. We have now developed liver-targeted nanoplexes by conjugating poly(amidoamine) (PAMAM) dendrimers with polyethylene glycol (PEG) and lactobionic acid (Gal) (PAMAM-PEG-Gal) which were complexed with AEG-1 siRNA (PAMAM-AEG-1si). The polymer conjugate was characterized by ^{1}H-NMR, MALDI, and mass spectrometry; and optimal nanoplex formulations were characterized for surface charge, size, and morphology. Orthotopic xenografts of human HCC cell QGY-7703 expressing luciferase (QGY-luc) were established in the livers of athymic nude mice and tumor development was monitored by bioluminescence imaging (BLI). Tumor-bearing mice were treated with PAMAM-siCon, PAMAM-siCon+ATRA, PAMAM-AEG-1si, and PAMAM-AEG-1si+ATRA. In the control group the tumor developed aggressively. ATRA showed little effect due to high AEG-1 levels in QGY-luc cells. PAMAM-AEG-1si showed significant reduction in tumor growth, and the combination of PAMAM-AEG-1si+ATRA showed profound and synergistic inhibition so that the tumors were almost undetectable by BLI. A marked decrease in AEG-1 level was observed in tumor samples treated with PAMAM-AEG-1si. The group treated with PAMAM-AEG-1si+ATRA nanoplexes showed increased necrosis, inhibition of proliferation, and increased apoptosis when compared to other groups. Liver is an ideal organ for RNAi therapy and ATRA is an approved anticancer agent. Our exciting observations suggest that the combinatorial approach might be an effective way to combat HCC.

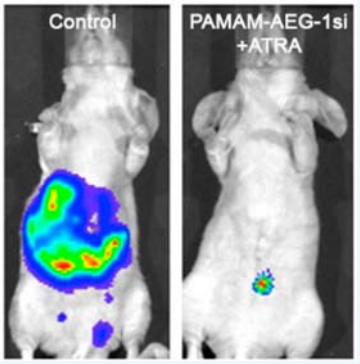

INTRODUCTION

Hepatocellular carcinoma (HCC) is a major global health problem. The incidence of HCC is increasing in the West, and it is the third highest cause of cancer-related death globally.[1] In the US, the estimated new cases of HCC for 2014 were 33 190, of which 23 000 were expected to die.[2] HCC, diagnosed at early stages, is amenable to potentially curative treatments, such as surgical therapies (resection and liver transplantation) and loco-regional procedures (radiofrequency ablation).[3,4] Five-year survival rates of up to 60−70% can be achieved in well-selected patients. However, disease that is diagnosed at an advanced stage or with progression after loco-regional therapy has a dismal prognosis, owing to the underlying liver disease and lack of effective treatment options. Sorafenib is the only FDA-approved drug for advanced HCC, which extends overall survival by only 2.8 months.[5] This dismal scenario mandates development and evaluation of novel therapeutic strategies for this fatal malady.

Astrocyte elevated gene-1 (AEG-1), also known as Metadherin (MTDH) and lysine-rich CEACAM-1 co-isolated (LYRIC), plays an important role in regulating hepatocarcinogenesis. We documented that AEG-1 is overexpressed in both mRNA and protein levels in a high percentage (>90%) of HCC patients and a significant percentage of patients harbored genomic amplification of the AEG-1 locus in chromosome 8q22.[6] AEG-1 is transcriptionally regulated by c-Myc,[7] an oncogene frequently upregulated in HCC.[8] The tumor suppressor miRNA miR-375, which is downregulated in HCC patients, targets AEG-1.[9] Thus, AEG-1 overexpression occurs by multiple mechanisms in HCC patients. HCC with more microvascular invasion or pathologic satellites, poorer differentiation, and TNM stages II to III are prone to exhibit higher

Received: May 4, 2015
Revised: June 11, 2015
Published: June 16, 2015

DOI: 10.1021/acs.bioconjchem.5b00254
Bioconjugate Chem. 2015, 26, 1651−1661

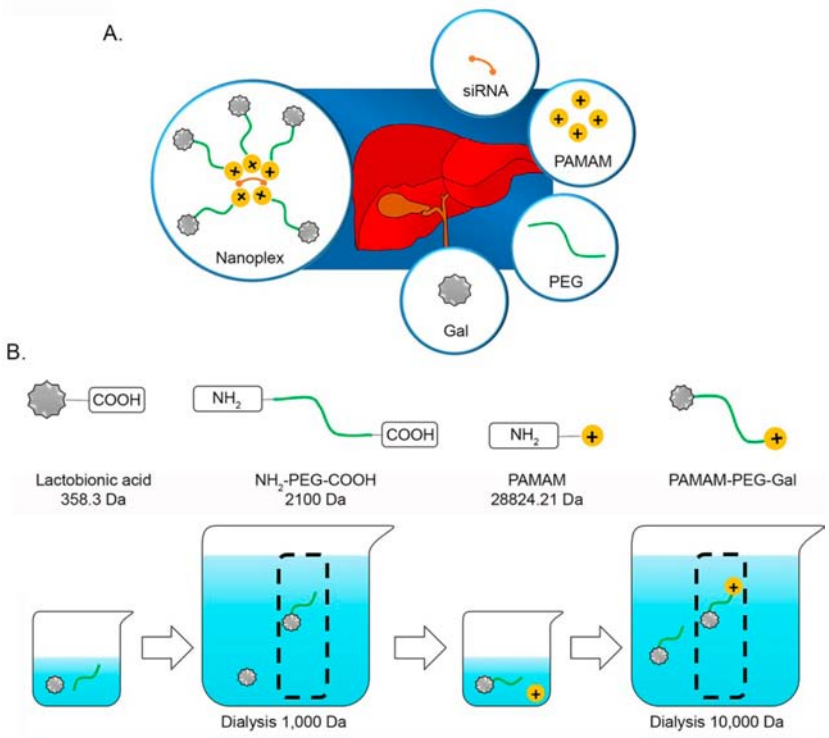

Figure 1. Generation of PAMAM-PEG-Gal. A. Strategy for targeting siRNA to liver. B. Strategy for preparation of the conjugates.

AEG-1 expression.[10] HCC patients with high AEG-1 expression documented higher recurrence and poor overall survival.[11] Overexpression of AEG-1 in poorly aggressive HCC cell line HepG3, which expresses a low level of AEG-1, significantly increases in vitro proliferation, invasion, and anchorage-independent growth and in vivo tumorigenesis, angiogenesis, and metastasis in nude mice.[6,12,13] As a corollary, transgenic mice with hepatocyte-specific overexpression of AEG-1 (Alb/AEG-1) develop highly aggressive angiogenic HCC with significantly accelerated kinetics upon treatment with the hepatocarcinogen n-nitrosodiethylamine (DEN) when compared to their wild-type counterparts.[14,15] Conversely, the knockdown of AEG-1 in highly aggressive human HCC cell line QGY-7703, expressing high levels of AEG-1, significantly abrogates in vivo tumorigenesis,[6,12] and an AEG-1 knockout (AEG-1KO) mouse shows profound resistance to DEN/phenobarbital (PB)-induced initiation and progression of HCC.[16] AEG-1 overexpression profoundly modulates expression of genes associated with proliferation, invasion, chemoresistance, angiogenesis, and metastasis in both human HCC cell lines and Alb/AEG-1 hepatocytes.[6,14,15] These studies establish an essential role of AEG-1 in hepatocarcinogenesis and identify AEG-1 as a valid target to develop a HCC therapeutic.

We have identified that AEG-1 interacts with retinoid x receptor (RXR) and inhibits retinoic acid (RA)-induced cytotoxicity.[17] AEG-1 contains an "LXXLL" motif which is employed by transcriptional coactivators, such as SRC-1, to interact with nuclear receptors to activate transcription.[18] In the absence of RA, the RXR-RAR heterodimer binds to co-repressors and inhibits transcription.[19] Upon binding of RA to RXR-RAR, there is a conformational change so that co-repressors move out allowing coactivators to bind and activate transcription. In the nucleus AEG-1 interacts with RXR via "LXXLL" motif and interferes with recruitment of coactivators thereby blocking RA-induced transcription.[17] In cancer cells AEG-1 accumulates in the cytoplasm and entraps RXR thereby preventing its nuclear translocation.[17] Additionally, AEG-1 induces phosphorylation-mediated inactivation of RXR by activating ERK.[17] Collectively, these mechanisms result in profound inhibition of RA function when AEG-1 is overexpressed. A combination of a lentivirus expressing AEG-1 shRNA (lenti.shAEG-1) and all-*trans* retinoic acid (ATRA) profoundly and synergistically inhibited growth of subcutaneous human HCC xenografts in nude mice.[17]

Nanoparticles have been proposed as potential means to deliver siRNA to cells. The benefits of nanoparticles include protection of siRNA, good tissue penetration, relatively good cell uptake, and stability.[20−24] Different types of compounds that can be collectively categorized as nanoparticles or nanoplexes have been tested for their ability to deliver nucleic acids to cells.[22] Cationic polymers can bind nucleic acids electrostatically and protect them from degradation, and can facilitate uptake to cells.[25,26] A promising class of cationic polymers that efficiently complex with siRNA is the poly(amidoamine) (PAMAM) dendrimers.[27−31] PAMAM dendrimers have a number of advantages over linear cationic polymers such as PEI.[30,32] In comparison to linear cationic polymers, PAMAM dendrimers are spherical, monodisperse polymers with a reduced structural density in the intramolecular core.[30] Additionally, PAMAM dendrimers also show very low toxicity profiles in mouse studies.[33] The use of PAMAM dendrimers is highly advantageous in gene delivery, but its high positive charge density results in a degree of cytotoxicity and hemolysis.[34,35] Addition of a PEG layer to PAMAM dendrimers reduces the charge density and thus significantly overcomes these drawbacks.[36,37] In addition, PEG is capable of enhancing the pharmacokinetics of the conjugate through increasing its circulation half-life by reducing interactions with serum proteins.[38] Although pegylation can

DOI: 10.1021/acs.bioconjchem.5b00254
Bioconjugate Chem. 2015, 26, 1651−1661

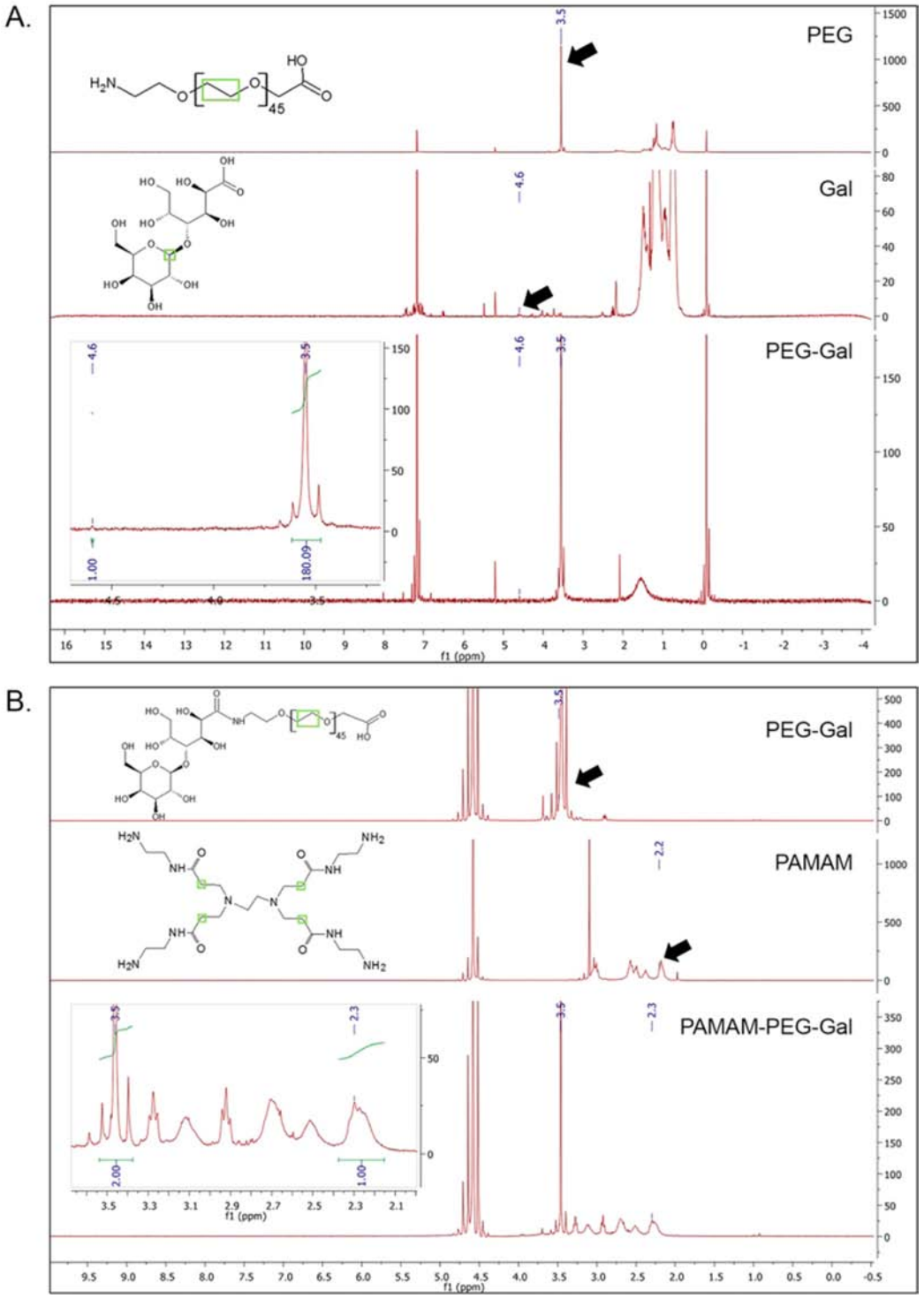

Figure 2. Characterization of PAMAM-PEG-Gal by ^{1}H NMR (300 MHz). A. ^{1}H NMR of PEG, Gal, and PEG-Gal using $CDCl_3$ as a solvent. Integral ratios between PEG (-C$\underline{H_2}$C$\underline{H_2}$O-) and Gal peaks are shown in the inset of the lower panel. B. ^{1}H NMR of PEG-Gal, PAMAM, and PAMAM-PEG-Gal using D_2O as a solvent. Integral ratios between PEG (-C$\underline{H_2}$C$\underline{H_2}$O-) and PAMAM (-C$\underline{H_2}$CONH-) peaks are shown in the inset of the lower panel. PAMAM structure demonstrated here is for generation zero, while the one utilized in the study is for generation five with 128 surface amine groups.

mitigate the drawbacks of using PAMAM dendrimers, it can also reduce its binding and uptake by targeted tissues (e.g., hepatocytes).[39] The addition of the lactobionic acid (Gal) to the PEG layer allows for a specific interaction of the nanoplex with asialoglycoprotien receptors that are overexpressed selectively in liver hepatocytes,[40] resulting in higher uptake of the nanoplexes in these cells. In this study, we document that hepatocyte-targeted nanoparticle-delivered AEG-1 siRNA in combination with ATRA results in profound synergistic inhibition of orthotopic human HCC xenografts in nude mice. These exciting observations suggest that this combinatorial strategy might be an effective way to counteract HCC.

DOI: 10.1021/acs.bioconjchem.5b00254
Bioconjugate Chem. 2015, 26, 1651−1661

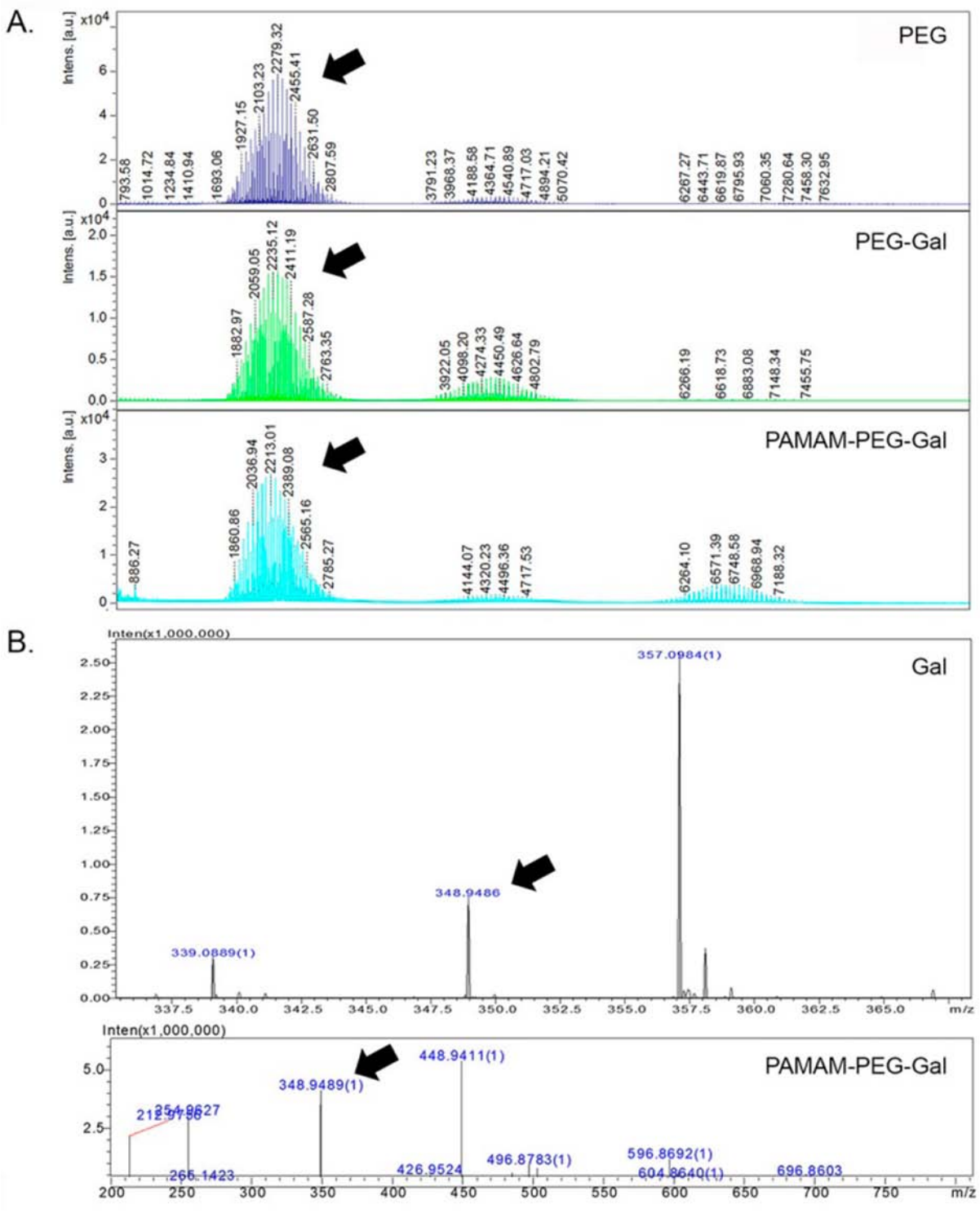

Figure 3. Characterization of PAMAM-PEG-Gal by MALDI and mass spectrometry. A. The presence of PEG in the final PAMAM-PEG-Gal construct was verified using MALDI. B. The presence of galactose ligands in the final PAMAM-PEG-Gal construct was verified using mass spectrometry.

RESULTS

Synthesis and Characterization of PAMAM-PEG-Gal.

For the specific purpose of the present studies, we have developed a delivery system for siRNA composed of poly(amidoamine) dendrimers (PAMAM), polyethylene glycol (PEG), and lactobionic acid (Gal) (Figure 1A). Cationic PAMAM complexes and compacts siRNA, PEG forms a hydrophilic layer outside of the polyplex for steric stabilization, and galactose serves as a cell binding ligand for liver cancer cells that overexpress the asialoglycoprotein receptor for galactose. The utilization of the PEG component and galactose (lactobionic acid) is expected to significantly improve the pharmacokinetics and tumor binding attributes of the delivery system and improve AEG-1 siRNA therapeutic efficiency. Synthesis of PAMAM-PEG-Gal was carried out utilizing EDC/

DOI: 10.1021/acs.bioconjchem.5b00254
Bioconjugate Chem. 2015, 26, 1651−1661

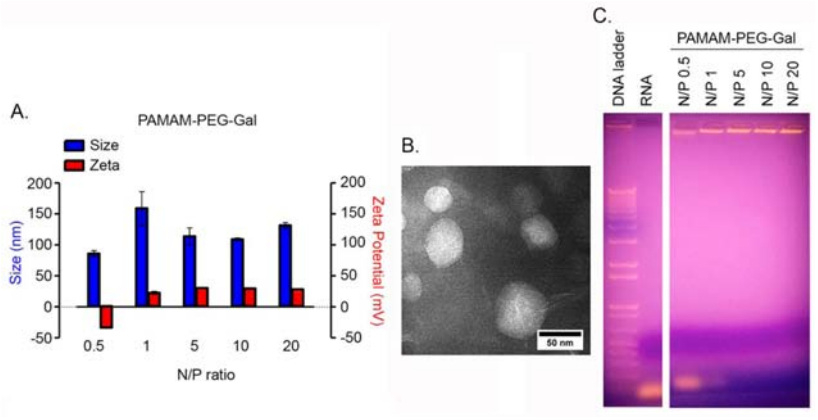

Figure 4. Characterization of the PAMAM-PEG-Gal complexed with AEG-1 siRNA (PAMAM-AEG-1si). A. Size and zeta potential measurements of PAMAM-PEG-Gal and AEG-1 siRNA complexes formed at varying amine to phosphate (N/P) ratios. B. Transmission electron microscopy image of N/P 20 showing spherical morphology and size of PAMAM-AEG-1si complexes. C. Gel electrophoresis assay showing siRNA retention in complexes prepared at varying N/P ratios.

NHS chemistry in a two-step process. First, the carboxylic group of Gal was conjugated to the amine group of PEG via an amide bond to form PEG-Gal. Second, the free carboxylic group of the PEG in PEG-Gal conjugate was further conjugated to the free amine groups in PAMAM via amide bonds to form PAMAM-PEG-Gal (Figure 1B). Molar ratios of PEG to Gal and PAMAM to PEG-Gal were further confirmed using ^{1}H-NMR spectroscopy (Figure 2). PEG, Gal, and PEG-Gal ^{1}H-NMR spectra in $CDCl_3$ are shown in (Figure 2A). Peaks at 3.5 and 4.5 ppm represented 180 H of PEG (-C$\underline{H_2}$C$\underline{H_2}$O-) and 1 H of Gal, respectively.[41,42] Integration ratios between both peaks at 3.5 and 4.5 ppm were 180.09:1 which confirmed that the molar ratio of PEG:Gal in the PEG-Gal conjugate was (180/180.09):(1/1) ≅ 1:1. It is worth noting here that $CDCl_3$ was utilized in this study because of the overlap that occurs between Gal peak at 4.5 ppm and the D_2O peak at 4.4−4.8, when D_2O was used as a solvent. PEG-Gal, PAMAM, and PAMAM-PEG-Gal ^{1}H-NMR spectra in D_2O are shown in (Figure 2B). Peaks at 2.3 and 3.5 ppm represented 504 H of PAMAM (-C$\underline{H_2}$CONH-) and 180 H of PEG-Gal (-C$\underline{H_2}$C$\underline{H_2}$O-), respectively.[43] PAMAM:PEG-Gal molar ratios in the PAMAM-PEG-Gal can also be calculated from the integration ratios between peaks at 2.3 and 3.5 ppm, which were equal to 1:2, respectively. These integration ratios showed that PAMAM:PEG-Gal molar ratios were (1/504):(2/180) ≅ 1:5.6, indicating that each molecule of PAMAM was conjugated to 5.6 molecule of PEG-Gal. The presence of PEG in the conjugates formed was further assessed through MALDI-TOF/TOF-MS (Figure 3A). MALDI spectrum showed peaks of mass around 2200 Da, and mass difference between adjacent peaks equivalent to multiples of PEG monomer (-CH_2CH_2O-, 44 Da). These peaks were observed in PEG, PEG-Gal, and PAMAM-PEG-Gal, supporting the presence of PEG in the final construct. Finally, the presence of Gal ligand in the final construct was further verified by IT-TOF-MS (Figure 3B). A distinct Gal peak of m/z 348.9 was found in the final construct of PAMAM-PEG-Gal, verifying the inclusion of Gal in the final construct and supporting the ^{1}H NMR data.

Characterization of PAMAM-AEG-1si Nanoplex. Complexes of PAMAM-PEG-Gal and AEG-1 siRNA were formed by electrostatic interactions at a series of different N/P ratios. Sizes of the prepared nanoplexes, at different N/P ratios, ranged between 85 and 158 nm in diameter. Increase in the size from 85 to 158 nm was observed when N/P ratio was increased from 0.5 to 1. Higher N/P ratios resulted in constant size of ∼120 nm (Figure 4A). The polydispersity index (PDI) values for each N/P ratio are presented in Table 1. The zeta potential of the formed nanoplexes changed drastically from −23.3 to +22.5 when N/P ratio changed from 0.5 to 1. N/P ratios of >1 resulted in a constant charge of ∼ +29.0 (Figure 4A). TEM analysis showed that complexes were spherical or semispherical in shape with porous but otherwise smooth surfaces (Figure 4B).The ability of the PAMAM-PEG-Gal to efficiently complex with siRNA at low N/P ratios was shown by gel retardation assays. siRNA complexed with PAMAM-PEG-Gal remained in the loading wells and did not migrate into an agarose matrix (1% w/v) at N/P ratios of >1 when an electric field was applied (Figure 4C).

Table 1. PDI Values at Each N/P Ratio

N/P ratio	PDI ± SD
0.5	0.103 ± 0.025
1	0.176 ± 0.019
5	0.093 ± 0.020
10	0.168 ± 0.004
20	0.225 ± 0.017

Combination of PAMAM-AEG-1si and ATRA Inhibits Orthotopic Human HCC Xenografts. QGY-7703 human HCC cells express high levels of AEG-1 and generate highly aggressive metastatic HCC in nude mice.[6,12] We have established stable clones of QGY-7703 cells expressing luciferase (QGY-luc).[44] QGY-luc cells were orthotopically implanted into the livers of athymic nude mice and tumor development was monitored by bioluminescence imaging (BLI) using Xenogen IVIS imager.[44] One week after the establishment of the tumor the mice (n = 8 per group) were treated with PAMAM-siCon, PAMAM-siCon+ATRA, PAMAM-AEG-1si, and PAMAM-AEG-1si+ATRA. ATRA was administered i.p. at a dose of 10 mg/kg and 5 μg of siRNA, conjugated with PAMAM-PEG-Gal at a ratio of 10:1, and was administered i.v. per injection. A total of 8 injections were administered twice a week and the mice were sacrificed 2 weeks after the last injection. In the control group the tumor developed aggressively (Figure 5A,B). ATRA showed very little

DOI: 10.1021/acs.bioconjchem.5b00254
Bioconjugate Chem. 2015, 26, 1651−1661

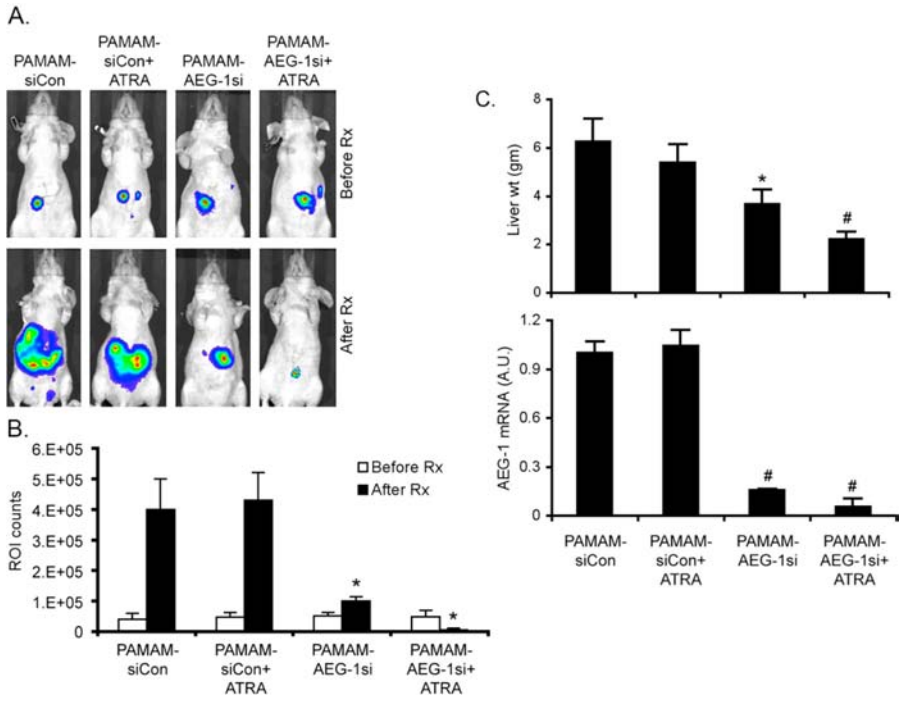

Figure 5. Combination of PAMAM-AEG-1si and ATRA profoundly inhibits orthotopic human HCC xenograft in nude mice. A. BLI imaging of the mice before and 2 wks after the last injection (After Rx). B. Quantification of photon counts from the animals. The data represent mean ± SEM; * $p < 0.01$ versus PAMAM-siCon. Eight animals per group were used. C. Liver weight at the end of the treatment (top panel). AEG-1 mRNA expression in the tumors at the end of the treatment by Taqman Q-RT-PCR (bottom panel). . The data represent mean ± SEM; * $p < 0.05$ and # $p < 0.01$ versus PAMAM-siCon.

effect which might be attributed to high AEG-1 level in QGY-luc cells. PAMAM-AEG-1si showed significant reduction in tumor growth and the combination of PAMAM-AEG-1si +ATRA showed profound and synergistic inhibition so that the tumors were almost undetectable by BLI (Figure 5A,B). Measurement of the liver weight at the end of the experiment corroborated the findings of BLI (Figure 5C, top panel). Analysis of AEG-1 mRNA in tumor samples by Taqman Q-RT-PCR showed marked decrease in AEG-1 level by PAMAM-AEG-1si when compared to the other groups (Figure 5C, bottom panel). Histologically, ATRA treatment did not show any significant difference from the control group (Figure 6A, top row). PAMAM-AEG-1si showed some areas of necrosis which might be attributed to inhibition of angiogenesis upon knockdown of AEG-1. The combination of PAMAM-AEG-1si +ATRA showed large areas of necrosis compared to other groups (Figure 6A, top row). There was marked decrease in AEG-1 expression with PAMAM-AEG-1si (Figure 6A, second row). It should be noted that this decrease in AEG-1 level was observed throughout the tumor indicating nearly 100% delivery of AEG-1 siRNA to the tumor tissue. Proliferation marker PCNA was markedly decreased in PAMAM-AEG-1si and with PAMAM-AEG-1si+ATRA the decrease was more pronounced (Figure 6A (third row), B). The PAMAM-AEG-1si group showed induction of apoptosis, determined by cleaved caspase-3 staining (Figure 6A (bottom row), B). However, it was markedly increased in the PAMAM-AEG-1si+ATRA group (Figure 6A (bottom row), B). The expression of ATRA-responsive genes RARB and HOXA1 in the tumor samples was checked at the end of the treatment. While ATRA and PAMAM-AEG-1si alone resulted in small but significant increases in these genes, the combination of PAMAM-AEG-1si+ATRA resulted in a robust increase in RARB and HOXA1 expression (Figure 6C). It should be noted that the growth rates of untreated QGY-luc cells and PAMAM-siCon group were similar (data not shown).

In parallel to checking therapeutic efficacy, we also checked for potential toxicity of the combinatorial treatment. No difference in body weight was observed in the mice of different groups throughout the course of treatment (Figure 7A). Histological analysis of PAMAM-AEG-1si+ATRA-treated QGY-luc tumor and adjacent normal liver at the end of the treatment clearly showed necrotic areas in the tumor with preservation of the architecture of the adjacent normal liver (Figure 7B). We also checked the acute effects of the combinatorial treatment 48 h after injection. No difference was observed in the levels of serum liver enzymes, namely, aspartate aminotransferase (AST), alanine aminotransferase (ALT), and alkaline phosphatase (Alk Phos); total protein, albumin, and globulin between control, PAMAM-AEG-1si, and PAMAM-AEG-1si+ATRA groups (Figure 7C). No increase in bilirubin level was detected following the combinatorial treatment. In all the groups, total bilirubin level was detected at ~0.1 mg/dL. Histological analysis of the liver also showed no signs of acute toxicity (Figure 7D).

■ DISCUSSION

We generated hepatocyte-targeted nanoparticles by successfully synthesizing PAMAM-PEG-Gal conjugate using EDC/NHS chemistry. ^{1}H NMR data showed that PEG:Gal molar ratios were ~1:1, and PEG:PAMAM ratios were ~5.6:1, indicating that 4.4% of the surface amine groups of PAMAM (fifth generation has 128 surface amine groups) were occupied. It is worth noting here that the targeted ratio of PEG:PAMAM of about 8% of the PAMAM surface amine groups was chosen because Qi et al. showed that higher transfection and acceptable

DOI: 10.1021/acs.bioconjchem.5b00254
Bioconjugate Chem. 2015, 26, 1651−1661

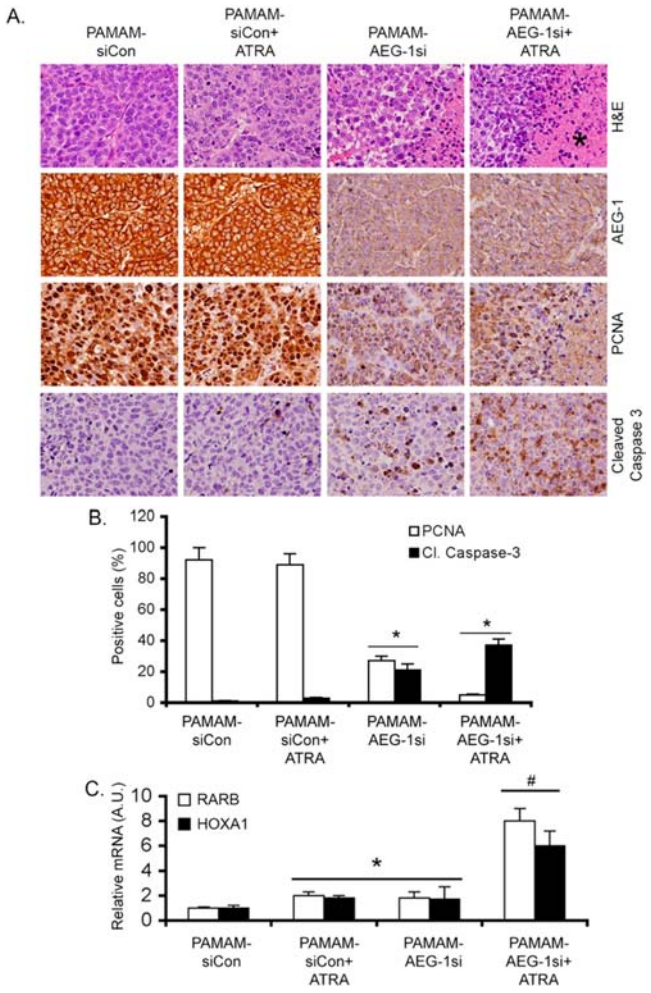

Figure 6. PAMAM-AEG-1si and ATRA combination inhibits proliferation and induces apoptosis. A. H&E (top row) and IHC staining of the tumors using the indicated antibodies. The asterisk indicates area of necrosis. B. Quantification of PCNA- and cleaved caspase-3 positive cells in the tumors. Data represent mean ± SEM *: $p < 0.01$ versus PAMAM-siCon. C. Expression of RARB and HOXA1 in the tumors at the end of the treatment by Taqman Q-RT-PCR. Data represent mean ± SEM * $p < 0.05$; # $p < 0.01$ versus PAMAM-siCon.

toxicity were achieved compared to 4% and 15%.[45] The presence of PEG and Gal in the final conjugate was further confirmed by MALDI and mass spectrometry. siRNA was complexed with the prepared conjugate through electrostatic interaction[46] between negatively charged phosphate groups of the siRNA and the positively charged amine groups of the PAMAM-PEG-Gal conjugate. TEM images of the prepared nanoplex after drying showed spherical nanoplexes of sizes around 50 nm. DLS measurements in an aqueous environment showed diameters of 131 nm, and this increase in hydrodynamic diameter from the DLS measurements further confirms the presence of hydrophilic PEG layers. An increase of the positive charge at higher N/P ratios indicates the condensation of the siRNA completely within the conjugate. This was confirmed using gel retardation assays in which nanoplexes prepared at N/P ratios of 0.5 and 1 showed migration of the siRNA band and this was completely hindered with nanoplexes prepared at higher N:P ratios. An N/P ratio of 10 was chosen for the in vivo experiments for the following reasons: (1) It is the lowest ratio that can condense the siRNA completely and thus higher protection of the siRNA from nucleases will be achieved.[46] (2) The smallest amount of PAMAM will be used and thus the lowest side effects are expected. (3) It was also shown that N/P ratios between 5 and 10 gave the most efficient transfection.[37]

We document that hepatocyte-targeted PAMAM dendrimers efficiently delivered AEG-1 siRNA to the target organ confirming the therapeutic utility of this delivery system in targeting AEG-1. Since any compound administered by i.v. first goes to the liver, HCC is the tumor that might derive the highest benefit from gene therapy strategies. A phase I trial for HCC employing i.v. administration of lipid nanoparticle (LNP)-conjugated siRNA for vascular endothelial growth factor (VEGF) and kinesin spindle protein (KSP) in cancer patients showed several beneficial aspects.[47] Biweekly administration was safe and well-tolerated. The siRNA effectively induced cleavage of targeted mRNA in the liver and demonstrated antitumor activity, including complete regression of metastatic lesion in the liver. This clinical trial, along with positive results from multiple preclinical studies targeting different molecules via nanoparticle-delivered siRNA, indicates that this modality of treatment is a viable option for HCC patients.[47−49] Indeed, the FDA has approved a recent clinical trial for nanoparticle-delivered PLK1 siRNA for HCC (http://investor.tekmirapharm.com/releasedetail.cfm?ReleaseID=850580). PAMAM-AEG-1si therefore is clinically relevant, especially in the context of HCC. Additionally, our studies, along with studies from various laboratories, have firmly established that AEG-1 positively regulates all aspects of aggressive cancer, and thus is a bona fide target for therapeutic intervention for a wide variety of cancer.[50] As such, PAMAM-AEG-1si, designed to target specific organs, might be of utility for tumors of other organ systems. AEG-1KO mice are viable and fertile,[16] further indicating that AEG-1 inhibition might be an effective anticancer strategy without causing harmful effects to normal cells.

Chemoresistance is one of the most profound phenotypes conferred by AEG-1, and indeed AEG-1 inhibition sensitizes killing by diverse therapeutic agents both in vitro and in nude mice xenograft models.[12,13] A variety of mechanisms, including translational upregulation of multidrug resistance gene-1 (MDR1) and upregulation of the transcription factor LSF, contribute to AEG-1-induced chemoresistance in HCC cells.[12,13] Our proposed combinatorial strategy is based on a molecular interaction between AEG-1 and RXR that we have unraveled and that confers resistance to RA-induced cytotoxicity.[17] We documented that ex vivo treatment of human HCC cells with lenti.shAEG-1 along with i.p. injection of ATRA resulted in synergistic and marked inhibition of subcutaneous xenografts in nude mice.[17] We now demonstrate that a PAMAM-AEG-1si and ATRA combination profoundly inhibits orthotopic xenografts in nude mice. These exciting findings from two independent experiments mandate that this strategy needs to be evaluated in a more stringent endogenous HCC model so that if found effective this strategy might be translated to the patients.

RA analogs have been evaluated in Phase II/III clinical trials for prevention and treatment of HCC.[51−53] These studies were carried out before AEG-1 was even cloned. One potential reason RA failed to progress further as a HCC therapeutic might be that overexpressed AEG-1 in a high percentage of HCC patients blocked RA action. ATRA is a routine cancer

DOI: 10.1021/acs.bioconjchem.5b00254
Bioconjugate Chem. 2015, 26, 1651−1661

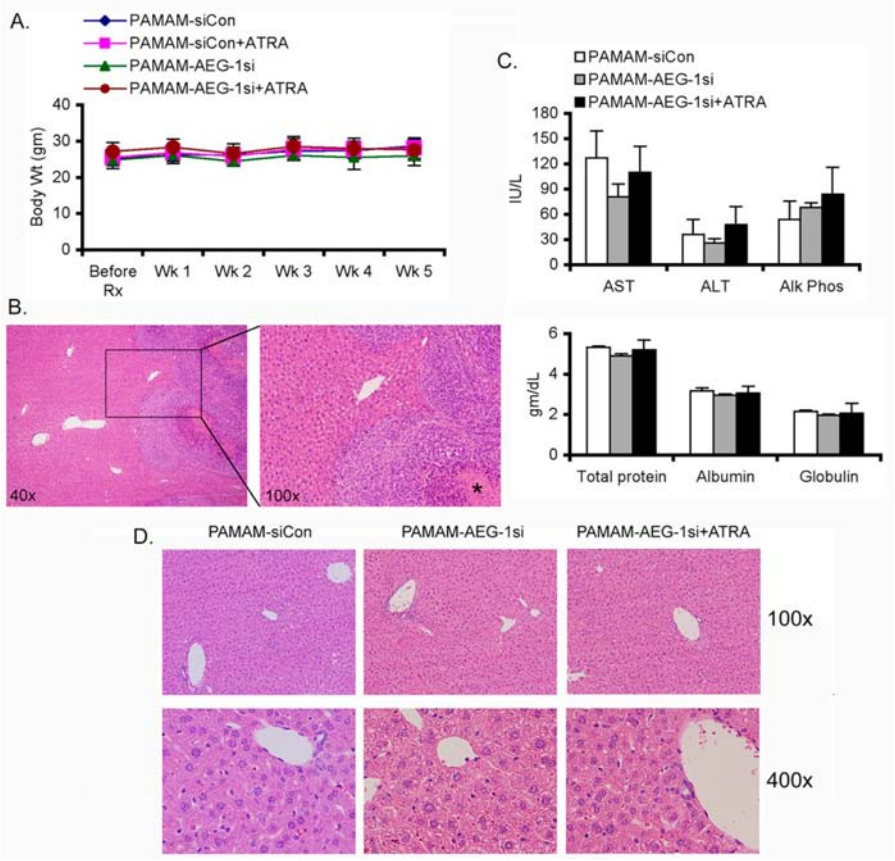

Figure 7. PAMAM-AEG-1si and ATRA combination does not induce toxicity. A. Body weight of the mice before, during, and after treatment. Wk 1 to 4 indicate treatment period. B. H&E staining of PAMAM-AEG-1si and ATRA-treated tumor and adjacent normal liver at the end of the treatment. Asterisk indicates necrosis. C. The indicated liver function parameters were measured in serum 48 h after injection. Data represent mean ± SEM (n = 3 per group). D. H&E staining of liver sections of the indicated treated group 48 h after injection.

therapeutic for leukemia.[54] Combination with AEG-1 inhibition might establish ATRA or other RA analogs again as a viable therapeutic option for HCC. The availability of a small molecule inhibitor for AEG-1 would have simplified AEG-1-targeting therapeutic strategies. However, AEG-1 is a scaffold protein which may not be amenable to inhibition by small molecules. Our proposed strategy of targeted nanoparticle-mediated siRNA delivery thus might be the most efficient way to inhibit AEG-1.

EXPERIMENTAL PROCEDURES

Materials. 2-[*N*-Morpholino] ethanesulfonic acid hydrate (MES) buffer, lactobionic acid, poly[ethylene glycol] 2-aminoethyl ether acetic acid, M_n 2100 (PEG), poly-[amidoamine], generation 5, provided as methanolic solution (PAMAM), 2-Mercapto ethanol, duterated water (D_2O), and duterated chloroform ($CDCl_3$) were purchased from Sigma-Aldrich (St. Louis, MO). 1-Ethyl-3-[3-(dimethylamino)propyl] carbodiimide hydrochloride (EDC) and *N*-hydroxysulfosuccinimide (sulfo-NHS) were purchased from Thermo Scientific (Rockford, IL). Sodium hydroxide (NaOH), acetonitrile (ACN), and formic acid were purchased from Fisher Scientific (Hampton, NH). Ultrapure DNase/RNase-free distilled water was purchased from Invitrogen (Grand Island, NY). A 0.22 μm syringe filter was purchased from Millex-GS (Millipore Corporation, Billerica, MA). Formvar 0.5% solution in ethylene dichloride film was purchased from Electron Microscopy Sciences (Hatfield, PA). Control scrambled siRNA (siCon) and AEG-1 siRNA were obtained from Sigma-Aldrich.

Generation of PAMAM-PEG-Gal. The PAMAM-PEG-Gal delivery system was constructed by conjugating galactose to one end of the polyethylene glycol (PEG) chain and the other end of the PEG chain was conjugated to the poly(amidoamine) (PAMAM) backbone (Figure 1). The first step in this synthesis was to prepare PEG-Gal. To do this, 5 mL of MES buffer (0.1 M, pH 6) was added to 45.65 mg of EDC (238 μmol = 10× lactobionic acid), 129.25 mg of sulfo-NHS (595 μmol = 2.5× EDC), and 8.53 mg of lactobionic acid (23.8 μmol = 10× PEG). This was then stirred for 15 min, 167.5 μL of 2-mercaptoethanol solution was added (2380 μmol = 10× EDC), and the pH was raised to 7 using 1 N NaOH solution. Next, 5 mg of NH_2-PEG-COOH (2.38 μmol) was added to the solution and stirred at room temperature overnight. Finally, the solution was dialyzed using a 1 kDa dialysis membrane against 1 L of distilled water for 48 h (water was changed at 2, 4, and 6 h), lyophilized (Freezone 4.5, Labconco Corp., Kansas City, MO), and stored at −20 °C. The next step was to use the PEG-Gal to prepare the PAMAM-PEG-Gal. To achieve this, 5 mL of 0.1 M MES buffer was added to 3.93 mg of EDC (20.50 μmol = 10× PEG-Gal), 11.13 mg of sulfo-NHS (51.26 μmol = 2.5× EDC), and 5 mg of PEG-Gal (2.050 μmol = 8% molar equivalent of the terminal amine groups in PAMAM,[45] and then stirred for 15 min.14.42 μL of 2-mercaptoethanol solution was added to quench free EDC[55] (205.0 μmol = 10× EDC) and the pH was raised to 7 using 1 N NaOH solution. 5.764 mg

DOI: 10.1021/acs.bioconjchem.5b00254
Bioconjugate Chem. 2015, 26, 1651−1661

of PAMAM (0.2 μmol = 25.63 μmole of amine groups) was then added to the solution and the solution was stirred at room temperature overnight. Finally, the solution was dialyzed using 10 kDa dialysis membrane against 1 L of distilled water for 48 h (water was changed at 2, 4, and 6 h), lyophilized for 2 days at −52 °C, and stored at −20 °C.

Preparation of the Nanoplexes. The nanoplexes were prepared by electrostatic interaction between positively charged PAMAM-PEG-Gal and negatively charged siRNA molecules. Nanoplexes were formulated at different ratios of primary amine groups in PAMAM-PEG-Gal to phosphate groups in siRNA (N/P ratios). PAMAM-PEG-Gal and siRNA solutions were prepared in ultrapure DNase/RNase-free distilled water. Solutions were sterilized by filtering with a 0.22 μm syringe filter. Finally, an equal volume of the desired concentration of cationic solution was pipetted into the anionic solution and then vortexed immediately for 30 s. The nanoplex solutions were incubated at room temperature for 30 min before use.

Characterization of PAMAM-PEG-Gal. *^{1}H-NMR.* Calculation of PEG to Gal molar ratio was performed by dissolving samples in $CDCl_3$, while the PAMAM-PEG ratio was calculated by dissolving samples in D_2O. Characterization was carried out using proton nuclear magnetic resonance (^{1}H NMR, Bruker Avance 300).

Matrix-Assisted Laser Desorption/Ionization Time-of-Flight/Time-of-Flight Mass Spectrometry (MALDI-TOF/TOF-MS). Estimation of the PEG presence in the conjugate was confirmed using MALDI-TOF/TOF-MS. Briefly, a matrix of α-cyano-4-hydroxycinnamic acid was dissolved in ACN and 0.1% formic acid at ratio of 50/50 (v/v), and then the matrix was mixed with an aqueous solution of the sample at a ratio of 1:1 (v/v). MALDI with positive, reflector mode was used. Mass spectra were acquired using a MALDI-TOF/TOF mass spectrometer (Ultraflextreme; Bruker).

Ion Trap and Time-of-Flight Mass Spectrometery (IT-TOF-MS). Gal presence in the conjugate was confirmed by injecting aqueous solutions of samples directly into IT-TOF-MS (Shimadzu, Columbia, MD) equipped with an electrospray ionization source in negative ion mode.

Characterization of Nanoplexes. *Size and Zeta Potential Measurements.* Particle size and zeta potential of nanoplexes (with varying N/P ratios) were measured using a Zetasizer Nano ZS particle analyzer via dynamic light scattering (DLS) technique (Malvern Instrument Ltd., Southborough, MA). Size and zeta potential measurements were performed on aqueous solution of the nanoplexes at 25 °C. Size was measured at 173° backscatter detection in disposable polystyrene cuvettes. Zeta potential was measured in a zeta potential folded capillary cell.

Transmission Electron Microscopy (TEM). Surface morphology of the prepared nanoplexes was assessed using TEM. A drop (10 μL) of aqueous solution of the nanoplexes (N/P 20) was added for 30 s on a carbon coated, glow discharged 400-mesh TEM copper grid that was precoated with a Formvar. Whatman filter paper was then used to remove any excess liquid and the grid was air-dried. Negative staining was then performed by adding a drop of freshly prepared 1% w/v phosphotungstic acid solution for 30 s followed by removing the excess stain as described before. TEM images were captured using JEOL JEM-1230 transmission electron microscope equipped with a Gatan UltraScan 1000 2k × 2k CCD acquisition system. Captured images were processed using *ImageJ* (Image Processing and Analysis in *Java* v 1.47).

Gel Electrophoresis. The ability of the conjugate to bind with siRNA was confirmed using gel electrophoresis assay. PAMAM-PEG-Gal and siRNA at N/P ratios of 0.5, 1, 5, 10, and 20 were mixed with 2× BlueJuice gel loading buffer (Invitrogen). The final solutions were loaded into the wells of a 1% (w/v) agarose gel containing 0.5 μg/mL of ethidium bromide in 1× Tris-acetate-EDTA (TAE) buffer. Gels were exposed to a constant current of 100 mA for 2 h. DNA migration was then visualized with a UV transilluminator (Spectroline, Westbury, NY).

Orthotopic Xenograft Studies in Nude Mice. All animal studies have been approved by the Institutional Animal Care and Use Committee (IACUC) of Virginia Commonwealth University. QGY-luc cells (QGY-7703 cells stably expressing luciferase) were orthotopically implanted by intrahepatic injection in athymic nude mice (6−8 weeks of age).[44] Tumor growth was monitored by bioluminescence imaging (BLI) with a Xenogen IVIS imager once a week.[44] For BLI, mice were injected with luciferin at a dose of 150 mg/kg i.p. After 10 min the mice were anesthetized using isoflurane and images were taken at an exposure time of 1 s. One week after the establishment of the tumor, the mice (n = 8 per group) were treated with PAMAM-siCon, PAMAM-siCon+ATRA, PAMAM-AEG-1si, and PAMAM-AEG-1si+ATRA. ATRA was administered i.p. at a dose of 10 mg/kg and 5 μg of siRNA, conjugated with PAMAM-PEG-Gal at a ratio of 10:1, was administered i.v. per injection. A total of 8 injections were administered twice a week and the mice were sacrificed 2 weeks after the last injection.

In Vivo Toxicity Studies. To check acute toxic effects of combinatorial therapy, C57/BL6 mice (n = 3) were injected with PAMAM-siCon, PAMAM-AEG-1si, and PAMAM-AEG-1si+ATRA at a dose described in the previous section. After 48 h mice were sacrificed, and blood and liver were collected for liver function test and histopathology, respectively, which were performed in the core facility of the Department of Pathology.

Immunohistochemistry. Immunohistochemistry was performed using formalin-fixed paraffin embedded (FFPE) sections as described previously.[13] The sections were blocked in PBST using 10% normal goat serum for rabbit polyclonal antibody, 10% normal horse serum for mouse monoclonal antibody, and 10% normal rabbit serum for chicken polyclonal antibody. Primary antibodies were diluted in PBST containing 5% corresponding blocking serum. The primary antibodies used were as follows: AEG-1 (chicken polyclonal; 1:500), PCNA and cleaved caspase-3 (cell signaling; mouse and rabbit monoclonal, respectively; 1:300). Secondary antibodies were diluted in PBST containing corresponding 2.5% blocking serum. The signals were developed by avidin-biotin-peroxidase complexes with a DAB substrate solution (Vector laboratories).

Total RNA Extraction, cDNA Preparation, and Quantitative RT-PCR. Total RNA was extracted from tumor samples using the QIAGEN miRNAeasy Mini Kit (QIAGEN, Hilden, Germany). cDNA preparation was done using ABI cDNA synthesis kit. Real-time polymerase chain reaction (RT-PCR) was performed using an ABI ViiA7 fast real-time PCR system and Taqman gene expression assays according to the manufacturer's protocol (Applied Biosystems, Foster City, CA).

Statistical Analysis. Data were represented as the mean ± standard error of mean (S.E.M.) and analyzed for statistical significance using one-way analysis of variance (ANOVA) followed by Newman-Keuls test as a post hoc test. A p-value of <0.05 was considered significant.

DOI: 10.1021/acs.bioconjchem.5b00254
Bioconjugate Chem. 2015, 26, 1651−1661

AUTHOR INFORMATION

Corresponding Authors

*E-mail: aliasger-salem@uiowa.edu. Tel: 319-335-8810. Fax: 319-335-9349.

*E-mail: dsarkar@vcu.edu. Tel: 804-827-2339. Fax: 804-628-1176.

Author Contributions

#Devaraja Rajasekaran, Jyoti Srivastava, and Kareem Ebeid contributed equally to the paper.

Notes

The authors declare no competing financial interest.

ACKNOWLEDGMENTS

The present study was supported in part by grants from The James S. McDonnell Foundation and National Cancer Institute Grant R01 CA138540 and R21 CA183954 (DS). C.L.R. is supported by a National Institute of Diabetes And Digestive And Kidney Diseases Grant T32DK007150. D.S. is the Harrison Endowed Scholar in Cancer Research and Blick Scholar. P.B.F. holds the Thelma Newmeyer Corman Chair in Cancer Research. A.K.S acknowledges support from the National Cancer Institute at the National Institutes of Health (P50 CA97274/UI Mayo Clinic Lymphoma SPORE grant and P30 CA086862 Cancer Center support grant) and the Lyle and Sharon Bighley Professorship. K.E. acknowledges the Egypt Ministry of Higher Education for a graduate fellowship award.

ABBREVIATIONS

AEG-1, astrocyte elevated gene-1; ATRA, all-*trans* retinoic acid; PAMAM, poly(amidoamine); PEG, polyethylene glycol; Gal, lactobionic acid

REFERENCES

(1) El-Serag, H. B. (2011) Hepatocellular carcinoma. *N. Engl. J. Med. 365*, 1118−1127.

(2) Siegel, R., Ma, J., Zou, Z., and Jemal, A. (2014) Cancer statistics, 2014. *CA Cancer J. Clin. 64*, 9−29.

(3) Llovet, J. M., and Bruix, J. (2008) Molecular targeted therapies in hepatocellular carcinoma. *Hepatology 48*, 1312−1327.

(4) Llovet, J. M., Burroughs, A., and Bruix, J. (2003) Hepatocellular carcinoma. *Lancet 362*, 1907−1917.

(5) Llovet, J. M., Ricci, S., Mazzaferro, V., Hilgard, P., Gane, E., Blanc, J. F., de Oliveira, A. C., Santoro, A., Raoul, J. L., Forner, A., et al. (2008) Sorafenib in advanced hepatocellular carcinoma. *N. Engl. J. Med. 359*, 378−390.

(6) Yoo, B. K., Emdad, L., Su, Z. Z., Villanueva, A., Chiang, D. Y., Mukhopadhyay, N. D., Mills, A. S., Waxman, S., Fisher, R. A., Llovet, J. M., et al. (2009) Astrocyte elevated gene-1 regulates hepatocellular carcinoma development and progression. *J. Clin. Invest. 119*, 465−477.

(7) Lee, S. G., Su, Z. Z., Emdad, L., Sarkar, D., and Fisher, P. B. (2006) Astrocyte elevated gene-1 (AEG-1) is a target gene of oncogenic Ha-ras requiring phosphatidylinositol 3-kinase and c-Myc. *Proc. Natl. Acad. Sci. U. S. A. 103*, 17390−17395.

(8) Villanueva, A., Newell, P., Chiang, D. Y., Friedman, S. L., and Llovet, J. M. (2007) Genomics and signaling pathways in hepatocellular carcinoma. *Semin. Liver Dis. 27*, 55−76.

(9) He, X. X., Chang, Y., Meng, F. Y., Wang, M. Y., Xie, Q. H., Tang, F., Li, P. Y., Song, Y. H., and Lin, J. S. (2012) MicroRNA-375 targets AEG-1 in hepatocellular carcinoma and suppresses liver cancer cell growth in vitro and in vivo. *Oncogene 31*, 3357−3369.

(10) Zhu, K., Dai, Z., Pan, Q., Wang, Z., Yang, G. H., Yu, L., Ding, Z. B., Shi, G. M., Ke, A. W., Yang, X. R., et al. (2011) Metadherin promotes hepatocellular carcinoma metastasis through induction of epithelial-mesenchymal transition. *Clin. Cancer Res. 17*, 7294−7302.

(11) Gong, Z., Liu, W., You, N., Wang, T., Wang, X., Lu, P., Zhao, G., Yang, P., Wang, D., and Dou, K. (2012) Prognostic significance of metadherin overexpression in hepatitis B virus-related hepatocellular carcinoma. *Oncol. Rep. 27*, 2073−2079.

(12) Yoo, B. K., Gredler, R., Vozhilla, N., Su, Z. Z., Chen, D., Forcier, T., Shah, K., Saxena, U., Hansen, U., Fisher, P. B., et al. (2009) Identification of genes conferring resistance to 5-fluorouracil. *Proc. Natl. Acad. Sci. U. S. A. 106*, 12938−12943.

(13) Yoo, B. K., Chen, D., Su, Z.-Z., Gredler, R., Yoo, J., Shah, K., Fisher, P. B., and Sarkar, D. (2010) Molecular mechanism of chemoresistance by Astrocyte Elevated Gene-1 (AEG-1). *Cancer Res. 70*, 3249−3258.

(14) Srivastava, J., Siddiq, A., Emdad, L., Santhekadur, P., Chen, D., Gredler, R., Shen, X.-N., Robertson, C. L., Dumur, C. I., Hylemon, P. B., et al. (2012) Astrocyte elevated gene-1 (AEG-1) promotes hepatocarcinogenesis: novel insights from a mouse model. *Hepatology 56*, 1782−1791.

(15) Srivastava, J., Siddiq, A., Gredler, R., Shen, X. N., Rajasekaran, D., Robertson, C. L., Subler, M. A., Windle, J. J., Dumur, C. I., Mukhopadhyay, N. D., et al. (2015) Astrocyte elevated gene-1 and c-Myc cooperate to promote hepatocarcinogenesis in mice. *Hepatology 61*, 915−929.

(16) Robertson, C. L., Srivastava, J., Siddiq, A., Gredler, R., Emdad, L., Rajasekaran, D., Akiel, M., Shen, X. N., Guo, C., Giashuddin, S., et al. (2014) Genetic deletion of AEG-1 prevents hepatocarcinogenesis. *Cancer Res. 74*, 6184−6193.

(17) Srivastava, J., Robertson, C. L., Rajasekaran, D., Gredler, R., Siddiq, A., Emdad, L., Mukhopadhyay, N. D., Ghosh, S., Hylemon, P. B., Gil, G., et al. (2014) AEG-1 regulates retinoid X receptor and inhibits retinoid signaling. *Cancer Res. 74*, 4364−4377.

(18) Heery, D. M., Kalkhoven, E., Hoare, S., and Parker, M. G. (1997) A signature motif in transcriptional co-activators mediates binding to nuclear receptors. *Nature 387*, 733−736.

(19) Mangelsdorf, D. J., Ong, E. S., Dyck, J. A., and Evans, R. M. (1990) Nuclear receptor that identifies a novel retinoic acid response pathway. *Nature 345*, 224−229.

(20) Kim, N., Jiang, D., Jacobi, A. M., Lennox, K. A., Rose, S. D., Behlke, M. A., and Salem, A. K. (2012) Synthesis and characterization of mannosylated pegylated polyethylenimine as a carrier for siRNA. *Int. J. Pharm. 427*, 123−133.

(21) Hong, L., Wei, N., Joshi, V., Yu, Y., Kim, N., Krishnamachari, Y., Zhang, Q., and Salem, A. K. (2012) Effects of glucocorticoid receptor small interfering RNA delivered using poly lactic-co-glycolic acid microparticles on proliferation and differentiation capabilities of human mesenchymal stromal cells. *Tissue Eng., Part A 18*, 775−784.

(22) Salem, A. K., Patil, S. D., and Burgess, D. J. (2012) Recent progress in non-viral nucleic acids delivery. *Int. J. Pharm. 427*, 1−2.

(23) Wu, L. P., Ficker, M., Christensen, J. B., Trohopoulos, P. N., and Moghimi, S. M. (2015) Dendrimers in medicine: therapeutic concepts and pharmaceutical challenges. *Bioconjugate Chem.*,.

(24) Leiro, V., Garcia, J. P., Tomas, H., and Pego, A. P. (2015) The present and the future of degradable dendrimers and derivatives in theranostics. *Bioconjugate Chem.*,.

(25) Intra, J., and Salem, A. K. (2008) Characterization of the transgene expression generated by branched and linear polyethylenimine-plasmid DNA nanoparticles in vitro and after intraperitoneal injection in vivo. *J. Controlled Release 130*, 129−138.

(26) Abbas, A. O., Donovan, M. D., and Salem, A. K. (2008) Formulating poly(lactide-co-glycolide) particles for plasmid DNA delivery. *J. Pharm. Sci. 97*, 2448−2461.

(27) Bielinska, A. U., Chen, C., Johnson, J., and Baker, J. R., Jr. (1999) DNA complexing with polyamidoamine dendrimers: implications for transfection. *Bioconjugate Chem. 10*, 843−850.

(28) Braun, C. S., Vetro, J. A., Tomalia, D. A., Koe, G. S., Koe, J. G., and Middaugh, C. R. (2005) Structure/function relationships of polyamidoamine/DNA dendrimers as gene delivery vehicles. *J. Pharm. Sci. 94*, 423−436.

DOI: 10.1021/acs.bioconjchem.5b00254
Bioconjugate Chem. 2015, 26, 1651−1661

(29) Cheng, Y., Xu, Z., Ma, M., and Xu, T. (2008) Dendrimers as drug carriers: applications in different routes of drug administration. *J. Pharm. Sci. 97*, 123−143.
(30) Esfand, R., and Tomalia, D. A. (2001) Poly(amidoamine) (PAMAM) dendrimers: from biomimicry to drug delivery and biomedical applications. *Drug Discovery Today 6*, 427−436.
(31) Liu, C., Liu, X., Rocchi, P., Qu, F., Iovanna, J. L., and Peng, L. (2014) Arginine-terminated generation 4 PAMAM dendrimer as an effective nanovector for functional siRNA delivery in vitro and in vivo. *Bioconjugate Chem. 25*, 521−532.
(32) Zhou, J., Wu, J., Hafdi, N., Behr, J. P., Erbacher, P., and Peng, L. (2006) PAMAM dendrimers for efficient siRNA delivery and potent gene silencing. *Chem. Commun. 22*, 2362−2364.
(33) Chauhan, A. S., Jain, N. K., and Diwan, P. V. (2010) Pre-clinical and behavioral toxicity profile of PAMAM dendrimers in mice. *Proc. R. Soc. London, Ser. A 466*, 1535−1550.
(34) Malik, N., Wiwattanapatapee, R., Klopsch, R., Lorenz, K., Frey, H., Weener, J. W., Meijer, E. W., Paulus, W., and Duncan, R. (2000) Dendrimers: relationship between structure and biocompatibility in vitro, and preliminary studies on the biodistribution of 125I-labelled polyamidoamine dendrimers in vivo. *J. Controlled Release 65*, 133−148.
(35) Fischer, D., Li, Y., Ahlemeyer, B., Krieglstein, J., and Kissel, T. (2003) In vitro cytotoxicity testing of polycations: influence of polymer structure on cell viability and hemolysis. *Biomaterials 24*, 1121−1131.
(36) Singh, P., Gupta, U., Asthana, A., and Jain, N. K. (2008) Folate and folate-PEG-PAMAM dendrimers: synthesis, characterization, and targeted anticancer drug delivery potential in tumor bearing mice. *Bioconjugate Chem. 19*, 2239−2252.
(37) Fant, K., Esbjorner, E. K., Jenkins, A., Grossel, M. C., Lincoln, P., and Norden, B. (2010) Effects of PEGylation and acetylation of PAMAM dendrimers on DNA binding, cytotoxicity and in vitro transfection efficiency. *Mol. Pharmaceutics 7*, 1734−1746.
(38) Lee, M., and Kim, S. W. (2005) Polyethylene Glycol-Conjugated Copolymers for Plasmid DNA Delivery. *Pharm. Res. 22*, 1−10.
(39) Chen, J., Gao, X., Hu, K., Pang, Z., Cai, J., Li, J., Wu, H., and Jiang, X. (2008) Galactose-poly(ethylene glycol)-polyethylenimine for improved lung gene transfer. *Biochem. Biophys. Res. Commun. 375*, 378−383.
(40) Jiang, H. L., Kwon, J. T., Kim, E. M., Kim, Y. K., Arote, R., Jere, D., Jeong, H. J., Jang, M. K., Nah, J. W., et al. (2008) Galactosylated poly(ethylene glycol)-chitosan-graft-polyethylenimine as a gene carrier for hepatocyte-targeting. *J. Controlled Release 131*, 150−157.
(41) Wang, Y., Su, J., Cai, W., Lu, P., Yuan, L., Jin, T., Chen, S., and Sheng, J. (2013) Hepatocyte-targeting gene transfer mediated by galactosylated poly(ethylene glycol)-graft-polyethylenimine derivative. *Drug Des. Dev. Ther. 7*, 211−221.
(42) Kim, E. M., Jeong, H. J., Park, I. K., Cho, C. S., Moon, H. B., Yu, D. Y., Bom, H. S., Sohn, M. H., and Oh, I. J. (2005) Asialoglycoprotein receptor targeted gene delivery using galactosylated polyethylenimine-graft-poly(ethylene glycol): in vitro and in vivo studies. *J. Controlled Release 108*, 557−567.
(43) Kim, T. I., Seo, H. J., Choi, J. S., Jang, H. S., Baek, J. U., Kim, K., and Park, J. S. (2004) PAMAM-PEG-PAMAM: novel triblock copolymer as a biocompatible and efficient gene delivery carrier. *Biomacromolecules 5*, 2487−2492.
(44) Chen, D., Siddiq, A., Emdad, L., Rajasekaran, D., Gredler, R., Shen, X.-N., Santhekadur, P., Srivastava, J., Robertson, C. L., Dmitriev, I., et al. (2013) Insulin-like growth factor binding protein-7 (IGFBP7): a promising gene therapeutic for hepatocellular carcinoma (HCC). *Mol. Ther. 21*, 758−766.
(45) Qi, R., Gao, Y., Tang, Y., He, R. R., Liu, T. L., He, Y., Sun, S., Li, B. Y., Li, Y. B., and Liu, G. (2009) PEG-conjugated PAMAM dendrimers mediate efficient intramuscular gene expression. *AAPS J. 11*, 395−405.
(46) Fant, K., Esbjorner, E. K., Lincoln, P., and Norden, B. (2008) DNA condensation by PAMAM dendrimers: self-assembly characteristics and effect on transcription. *Biochemistry 47*, 1732−1740.
(47) Tabernero, J., Shapiro, G. I., LoRusso, P. M., Cervantes, A., Schwartz, G. K., Weiss, G. J., Paz-Ares, L., Cho, D. C., Infante, J. R., Alsina, M., et al. (2013) First-in-humans trial of an RNA interference therapeutic targeting VEGF and KSP in cancer patients with liver involvement. *Cancer Discovery 3*, 406−417.
(48) Bogorad, R. L., Yin, H., Zeigerer, A., Nonaka, H., Ruda, V. M., Zerial, M., Anderson, D. G., and Koteliansky, V. (2014) Nanoparticle-formulated siRNA targeting integrins inhibits hepatocellular carcinoma progression in mice. *Nat. Commun. 5*, 3869.
(49) Dudek, H., Wong, D. H., Arvan, R., Shah, A., Wortham, K., Ying, B., Diwanji, R., Zhou, W., Holmes, B., Yang, H., et al. (2014) Knockdown of beta-catenin with dicer-substrate siRNAs reduces liver tumor burden in vivo. *Mol. Ther. 22*, 92−101.
(50) Sarkar, D., and Fisher, P. B. (2013) AEG-1/MTDH/LYRIC: Clinical Significance. *Adv. Cancer Res. 120*, 39−74.
(51) Muto, Y., Moriwaki, H., Ninomiya, M., Adachi, S., Saito, A., Takasaki, K. T., Tanaka, T., Tsurumi, K., Okuno, M., Tomita, E., et al. (1996) Prevention of second primary tumors by an acyclic retinoid, polyprenoic acid, in patients with hepatocellular carcinoma. Hepatoma Prevention Study Group. *N. Engl. J. Med. 334*, 1561−1567.
(52) Muto, Y., Moriwaki, H., and Saito, A. (1999) Prevention of second primary tumors by an acyclic retinoid in patients with hepatocellular carcinoma. *N. Engl. J. Med. 340*, 1046−1047.
(53) Takai, K., Okuno, M., Yasuda, I., Matsushima-Nishiwaki, R., Uematsu, T., Tsurumi, H., Shiratori, Y., Muto, Y., and Moriwaki, H. (2005) Prevention of second primary tumors by an acyclic retinoid in patients with hepatocellular carcinoma. Updated analysis of the long-term follow-up data. *Intervirology 48*, 39−45.
(54) Sanz, M. A., and Lo-Coco, F. (2011) Modern approaches to treating acute promyelocytic leukemia. *J. Clin. Oncol. 29*, 495−503.
(55) Xu, J., Ruchala, P., Ebenstain, Y., Li, J. J., and Weiss, S. (2012) Stable, compact, bright biofunctional quantum dots with improved peptide coating. *J. Phys. Chem. B 116*, 11370−11378.

DOI: 10.1021/acs.bioconjchem.5b00254
Bioconjugate Chem. 2015, 26, 1651−1661